DALTON

Synthesis, structure, magnetic, spectroscopic and electrochemical behaviour of chloro-iron(III) and -manganese(III) complexes of 2,3,7,8,12,13,17,18-octakis(ethylsulfanyl)-5,10,15,20-tetraazaporphyrin †

Giampaolo Ricciardi,[a] Alfonso Bavoso,[a] Alessandro Bencini,[b] Angela Rosa,[a] Francesco Lelj*,[a] and Francesca Bonosi[c]

[a] *Dipartimento di Chimica, Università della Basilicata, Via N. Sauro 85, 85100 Potenza, Italy*
[b] *Dipartimento di Chimica, Università di Firenze, Via Maragliano 77, 50144 Firenze, Italy*
[c] *Dipartimento di Chimica, Università di Firenze, Via G. Capponi 9, 50121 Firenze, Italy*

The complexes [M(oespz)Cl] [M = Mn^{III} or Fe^{III}; oespz = 2,3,7,8,12,13,17,18-octakis(ethylsulfanyl)-5,10,15,20-tetraazaporphyrinate dianion] have been prepared and their structures determined. The isomorphous structures consist of stacked dimers. Monomers, within each dimer, are slipped and faced in *trans* fashion respect to the M–Cl bond. Weak interdimer interactions arise from Cl · · · S contacts. Intradimer interactions are provided by relatively long M · · · S and N (pyrrole) · · · S contacts. Magnetic susceptibility measurements revealed that [Mn(oespz)Cl] is a high-spin ($S = 2$) complex with weak antiferromagnetic coupling between the Mn^{III}. The toluene frozen-glass EPR spectrum of [Fe(oespz)Cl] seems to be consistent with a $S = \frac{3}{2}$ ground state, whereas the polycrystalline powder EPR spectrum at 4.2 K and magnetic susceptibility data are better rationalized in terms of a $S = \frac{5}{2}$ and $\frac{1}{2}$ admixture. The crowding of the UV/VIS spectra of both complexes and the red shift of the Soret and Q bands of [Fe(oespz)Cl] are related to the effects of the peripheral ethylsulfanyl groups on the porphyrazinato ring. Both compounds show characteristic NIR absorptions. Voltammetric data are consistent with the tendency of the porphyrazinate ligand to stabilize the lower oxidation states of metals relative to phthalocyanines and porphyrins.

The chemical and physical properties of transition-metal porphyrazines (azaporphyrins) have attracted considerable interest.[1,2] They show a rich co-ordination chemistry and quite unusual magnetic and spectroscopic behaviour. Moreover, there is evidence that the porphyrazinate dianion, due to its particularly effective π-acceptor ability, tends to stabilize lower metal oxidation states (*i.e.* Fe^{II} *vs.* Fe^{III}, Co^{II} *vs.* Co^{III}) relative to porphyrinate ligand, which makes its complexes attractive catalysts.[2a,3]

Metalloporphyrazines peripherally substituted with thioether groups are of particular interest.[2d,k] The modifications induced by the thioether substituents on the porphyrazinato framework are reflected in the spectroscopic properties of these metallomacrocycles.[1,2] In addition, the thioether groups provide new in-[2d] and out-of-plane peripheral co-ordination sites. The chemical flexibility inherent in the octa(alkylsulfanyl)-porphyrazine derivatives of transition metals and lanthanides is probably the origin of the appealing thermodynamic and spectroscopic behaviour of low-dimensional organized molecular assemblies such as discotic liquid crystals and Langmuir–Blodgett films based on these complexes.[2f,k]

It is however rather unfortunate that most metallo-octa(alkylsulfanyl)porphyrazines crystallize in a fibre-like habit which is unsuitable for single-crystal X-ray diffraction. This prevents a thorough understanding of the nature of the intermolecular interactions (*i.e.* metal–metal, metal–ligand and/or ligand–ligand) occurring in the condensed phase. Actually, only the structures of [Mg(omspz)(H_2O)] (omspz = 2,3,7,8,12,13,17,18-octakis(methylsulfanyl)-5,10,15,20-tetra-azaporphyrinate) and Sn_4-*star*-M(porphyrazine)S_8 (M = Ni^{II} or Cu^{II}) have been solved.[2e] In these systems the strong molecular association phenomena which usually induce fibre-like crystal growth are much weaker. In fact, the fifth axial ligand in [Mg(omspz)(H_2O)], and, respectively, the capping bulky dialkyltin(IV) groups in nickel and copper *star*-porphyrazines prevent close approach of the porphyrazine octathiolate rings.

In order to highlight the relevant structural features of this class of complexes we decided to investigate the chloroiron(III)- and chloromanganese(III)–porphyrazines [Fe^{III}(oespz)Cl] and [Mn^{III}(oespz)Cl] (oespz = 2,3,7,8,12,13,17,18-octakis(ethylsulfanyl)-5,10,15,20-tetraazaporphyrinate). The choice of these complexes was based on the following considerations. The axial chloride ligand may play the same role as the H_2O ligand in [Mg(omspz)(H_2O)], leading to X-ray-quality crystals; unlike Mg^{II} in [Mg(omspz)(H_2O)], however, five-co-ordinated manganese(III) and iron(III) are co-ordinatively unsaturated in the tetraazamacrocyclic environment, and may further interact with a sixth axial ligand;[4] this makes these complexes especially suitable for studying the intermolecular interactions involving the metal. Five-co-ordination lowers the reactivity at the metal centres making these compounds also ideal building blocks for organized molecular systems.[5]

In this paper the synthesis, crystal and molecular structure, magnetic behaviour, UV/VIS and near-infrared (NIR) electronic spectra, cyclic voltammetric response and EPR spectra of these complexes are investigated. These physico-chemical properties are of interest in view of the use of these compounds as building blocks for new materials. The similarities to and differences from the unsubstituted analogues and the corresponding complexes of unsubstituted porphyrin (H_2por) and phthalocyanine (H_2pc), are also discussed, whenever possible.

Experimental

Materials

All chemicals and solvents (Aldrich Chemicals Ltd.) were of

† *Non-SI unit employed:* $\mu_B \approx 9.27 \times 10^{-24}$ J T^{-1}.

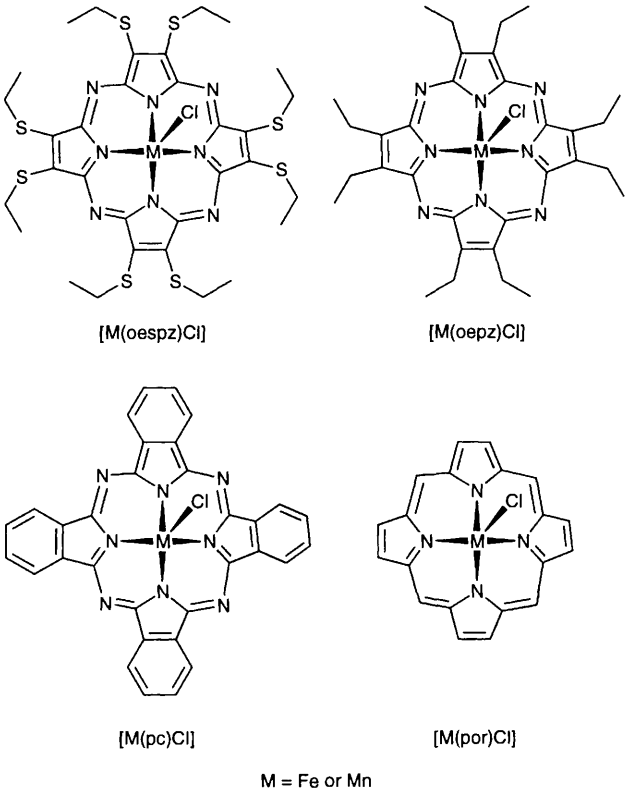

reagent grade used as supplied. Solvents used in physical measurements were of spectroscopic or HPLC grade. Anhydrous $FeBr_3$, $Fe(O_2CMe)_2$ and $Mn(O_2CMe)_2$ were obtained from Strem. Anhydrous ethanol and dimethylformamide (dmf) were obtained according to the literature procedures.[6] Silica gel used for chromatography was Merck Kieselgel 60 (270–400 mesh). Chloromanganese(III) phthalocyaninate was from Aldrich. Dichloromethane for voltammetric studies was refluxed under nitrogen with CaH_2 for at least 48 h and stored over 4 Å molecular sieves. The salts $[NBu^n_4]Cl$, $[NBu^n_4][ClO_4]$ and $[NBu^n_4][BF_4]$ were recrystallized from ethanol and dried under mild vacuum. Air- and moisture-sensitive chemicals were handled under an inert nitrogen atmosphere using standard Schlenk techniques or in a laboratory-made glove-box.

Physical measurements

Microanalyses were performed by the Analytische Laboratorien of Professor H. Malissa and G. Reuter Gmbh, Gummersbach, Germany and at the Engineering Department, University of Basilicata. Infrared spectra were run as KBr discs on a 5PC Nicolet FT-IR spectrometer over the range 400–4000 cm^{-1}, fast atom bombardment (FAB) mass spectra on a VG ZAB 2SE double-focusing mass spectrometer equipped with a caesium gun operating at 25 kV (2 mA) using a 3-nitrobenzyl alcohol matrix, solution electronic spectra in 1 or 10 cm path length quartz cells in the region 200–2500 nm on a UV-VIS-NIR 05E Cary spectrophotometer and proton ^1H NMR spectra on an AM 300 MHz Bruker spectrometer. Toluene solution frozen-glass X-band EPR spectra were recorded with a Bruker 200D ESR spectrometer. The temperature was varied with the Bruker 100/700 ST accessory. Polycrystalline powder EPR spectra were measured in the range 4.2–300 K using a Varian E-9 spectrometer. Liquid-helium temperature was reached with an ESR90 cryostat (Oxford Instruments). In a typical experiment the instrument settings were: modulation frequency, 100 kHz; modulation amplitude, 0.5 G (0.5×10^{-4} T); receiver gain, 6.2×10^2; microwave power, 10 mW. Variable-temperature magnetic measurements were made in the range 2.5–270 K using a Metronique Ingegnieric SQUID apparatus.

Electrochemical measurements were performed with an EG&G Princeton Applied Research (PAR) potentiostat/galvanostat, model 273, or with an AMEL 5000 system, in conjunction with a Linseis X-Y recorder; for all readings a three-electrode system in CH_2Cl_2 containing 0.1 mol dm^{-3} supporting electrolyte was employed. Cyclic voltammetric measurements were obtained with a double-platinum electrode and a Ag–AgCl reference electrode equipped with a Luggin capillary under an atmosphere of purified N_2.

Syntheses

The compound H_2oespz was synthesized using the procedure described for analogous alkylsulfanyl porphyrazines.[2d–k] The crude product was carefully purified by flash chromatography on silica gel (first band) using CH_2Cl_2–hexane (1:1) as eluent (Found: C, 48.25; H, 5.25; N, 14.00; S, 32.15. $C_{32}H_{42}N_8S_8$ requires C, 48.35; H, 5.30; N, 14.10; S, 32.25%). ^1H NMR (300 MHz, $CDCl_3$) δ_H −0.95 (2 H), 1.52 (24 H, t) and 4.25 (24 H, q). UV/VIS (CH_2Cl_2): λ 360 (log ε 4.67) (Soret), 490 (4.17), 520 (4.18), 632 (4.58), 670 (sh) (4.56), 655 (4.60) and 715 nm (4.81) (Q bands). FAB mass spectrum (positive-ion mode): m/z = 794, cluster, M^+ (calc. 794).

[Mn(oespz)]. In an inert-atmosphere glove-box, H_2oespz (0.100 g, 0.13 mmol) and $Mn(O_2CMe)$ (0.035 g, 0.20 mmol) in refluxing dry EtOH (10 cm^3) led, in 24 h, to a dark blue solution which, after freezing at −70 °C overnight, filtration and washing with hexane afforded metallic needle-like crystals of [Mn(oespz)] (yield ≈70%) (Found: C, 45.50; H, 4.35; N, 13.55; S, 30.15. $C_{32}H_{40}MnN_8S_8$ requires C, 45.30; H, 4.75; N, 13.20; S, 30.25%). UV/VIS (EtOH): λ 280 (log ε 4.28), 345 (4.37) (Soret), 420 (3.96), 450 (3.92), 590 (4.40), 640 (4.18) and 720 nm (4.09) (Q bands).

[Mn(oespz)Cl]. Layering MeOH or EtOH (10 cm^3) over a solution of [Mn(oespz)] (1 mol dm^{-3}) in Bu^nCl (20 cm^3) at room temperature gave after evaporation of the solvent mixture, within 3–5 d regular dark red platelets of [Mn(oespz)Cl] (yield >90%) (Found: C, 43.25; H, 4.50; Cl, 4.00; N, 12.75; S, 29.15. $C_{32}H_{40}ClMnN_8S_8$ requires C, 43.50; H, 4.55; Cl, 4.00; N, 12.70; S, 29.05%). FAB mass spectrum (positive-ion mode): m/z = 847, cluster, $[M - Cl]^+$ (calc. 847); 1694, cluster, $[dimer - 2Cl]^+$ (calc. 1694); 1709, cluster, $[dimer - Mn]^+$ (calc. 1709); and 1729, cluster, $[dimer - Cl]^+$ (calc. 1729).

[{Fe(oespz)}$_2$O]. To a slurry of H_2oespz (0.200 g, 0.25 mmol) in 2-chloroethanol (30 cm^3) were added *sym*-2,4,6-trimethylpyridine (*ca.* 0.5 cm^3) and $FeBr_3$ (0.090 g, 0.30 mmol) dissolved in 5 cm^3 of the same solvent. The mixture was allowed to reflux for 24 h under nitrogen and, subsequently, for 1 h in the open air. The solution turned from green-blue to blue-grey. The mixture after drying *in vacuo* afforded a dark deliquescent solid. Purification by chromatography on silica gel using CH_2Cl_2–EtOH (4:1) as eluent afforded 0.190 g of [{Fe(oespz)}$_2$O] (yield ≈90%). UV/VIS (CH_2Cl_2). (λ_{max}), 248 (log ε 4.30), 292 (4.11), 320 (sh) (3.96), 384 (4.37), 416 (sh) (4.08), 624 (3.00), 644 (3.10) and 660 (3.00) (Found: C, 44.95; H, 4.65; N, 12.65; S, 29.50. $C_{64}H_{80}Fe_2N_{16}OS_{16}$ requires C, 44.85; H, 4.70; N, 13.05; S, 29.95%).

[Fe(oespz)Cl]. The complex [{Fe(oespz)}$_2$O] (0.100 g) dissolved in CH_2Cl_2 (50 cm^3) was shaken with 0.1 mol dm^{-3} HCl aqueous solution (100 cm^3) in a separatory funnel. After 12 h the dichloromethane solution was dried over Na_2SO_4 and filtered on Celite. The volume was reduced to ≈20 cm^3 and pentane (15 cm^3) was added. Slow evaporation of the red mixture at room temperature afforded within a week 0.090 g of dark red crystals of [Fe(oespz)Cl] suitable for X-ray

investigations (yield 90%) (Found: C, 43.95; H, 4.60; Cl, 3.85; N, 12.45; S, 28.40. $C_{32}H_{40}ClFeN_8S_8$ requires C, 43.45; H, 4.55; Cl, 4.00; N, 12.65; S, 29.00%). FAB mass spectrum (positive-ion mode): m/z = 848, cluster, $[M - Cl]^+$ (calc. 848); 1696, cluster, [dimer − 2Cl]$^+$ (calc. 1696); 1710, cluster, [dimer − Fe]$^+$ (calc. 1710); 1731, cluster, [dimer − Cl]$^+$ (calc. 1731).

Crystallography

Crystal data, details of data collection and refined parameters for [Mn(oespz)Cl] and [Fe(oespz)Cl] are given in Table 1. Selected bond lengths and angles in Tables 2 and 3.

[Mn(oespz)Cl]. All data were collected at room temperature on an Enraf-Nonius CAD-4 diffractometer using graphite-monochromated Cu-Kα radiation (λ 1.541 84 Å). The unit cell was determined from 25 well centred reflections. The intensity data were collected in an ω–2θ scan mode. A total of 7168 reflections were measured to θ_{max} = 69°; 3097 with $I > 3\sigma(I)$ were used. Data reduction included correction for background and Lorentz-polarization effects. An absorption correction was applied according to ref. 7. The intensities of two reflections were measured every hour during data collection as a check of the stability of the diffractometer and the crystal; no appreciable decay in intensities was observed. The crystal orientation was checked every 200 intensity measurements using two control reflections.

[Fe(oespz)Cl]. The data were collected as above. A total of 7168 reflections were measured to θ_{max} = 70°; 3266 having $I > 3\sigma(I)$ were used. Data were processed as for [Mn(oespz)Cl].

Structure analysis and refinement. The structures were solved by direct methods using MULTAN.[8] The analysis of the E map derived from the set of phases with the best combined figure of merit revealed the positions of most non-hydrogen atoms. In both cases the remaining atoms were located from succeeding Fourier syntheses. The structures were refined (on F) anisotropically by full-matrix least-squares procedures to an R value of 0.055 (R' = 0.059) for [Mn(oespz)Cl] and to R 0.056 (R' = 0.059) for [Fe(oespz)Cl]. The function minimized was $\Sigma w (|F_o| - |F_c|)^2$, with w = 1 for all the observed $I > 3\sigma(I)$ reflections. Hydrogen atoms, included in the structural model in stereochemically calculated positions, were refined but restrained to ride on the atoms to which they are bonded. Atomic scattering factors and anomalous dispersion corrections were taken from ref. 9. All the computations were performed by the MOLEN package[10] running on a DEC VAX 6510 computer.

Atomic coordinates, thermal parameters and bond lengths and angles have been deposited at the Cambridge Crystallographic Data Centre (CCDC). See Instructions for Authors, *J. Chem. Soc., Dalton Trans.*, 1996, Issue 1. Any request to the CCDC for this material should quote the full literature citation and the reference number 186/58.

Results and Discussion

Syntheses

The only manganese porphyrazine known is the highly insoluble [Mn^{II}(oppz)] (oppz = octaphenylporphyrazinate) which was prepared in ≈5.7% yield in 1985.[11] We have now succeeded in preparing [Mn(oespz)] and [Mn(oespz)Cl] in high yield, starting from the highly soluble H_2oespz. Treatment of [Mn(oespz)] with alkyl chlorides affords the [Mn(oespz)Cl] complex, according to reaction (1). Direct

$$2[Mn(oespz)] + 2RCl \longrightarrow 2[Mn(oespz)Cl] + R\text{–}R \quad (1)$$

mixing of the reagents in equimolar amounts rapidly leads to the formation of a dark red vitreous precipitate. However, layering ethanol or methanol over a dilute red solution of [Mn(oespz)] in RCl (R = $CHCl_2$, CH_2Cl or Bu^n) gave dark red crystals of [Mn(oespz)Cl] suitable for X-ray investigations in 3–7 d, the formation of the alkane being easily monitored through ^{1}H NMR spectroscopy. No significant amounts of the manganese σ-alkylated product were detected by ^{1}H NMR spectroscopy, indicating that the combination of [Mn(oespz)] with the alkyl radicals is too slow compared to the one-electron oxidative addition of the Cl$^\bullet$ radical. It is remarkable that the reaction of [Mn(oespz)] with RCl only involves chlorine-atom abstraction. It is well established, that the reaction of porphyrin-like metallomacrocycles such as cobalt(II) Shiff bases or cobalt(II) porphyrins,[12] electroreductively generated iron(I) porphyrins,[13] or [{Rh(oepz)}$_2$] dimer[14] with alkyl halides predominantly leads to σ alkylation of the metal centre. Thus the reaction of [Mn(oespz)] with alkyl chlorides strongly resembles the halogen-atom abstraction from RX (X = Cl, Br or I) by transition-metal radicals.[15] The synthesis of [Fe(oespz)Cl] was carried out according to steps (2) and (3).

$$H_2oespz \xrightarrow[sym\text{-}NC_5H_2Me_3\text{-}2,4,6,\ O_2]{ClC_2H_4OH} [\{Fe(oespz)\}_2O] \quad (2)$$

$$[\{Fe(oespz)\}_2O] \xrightarrow[CH_2Cl_2]{water,\ HCl} [Fe(oespz)Cl] \quad (3)$$

Reaction of H_2oespz with a slight molar excess of anhydrous $FeBr_3$ or $Fe(O_2CMe)_2$ in the presence of the sterically hindered base 2,4,6-trimethylpyridine and, subsequently, with O_2, affords a deep blue-grey solution, from which an air-stable dark deliquescent solid was isolated in quantitative yield. On the basis of spectroscopic and microanalytical data this was formulated as the μ-oxo dimer [{Fe(oespz)}$_2$O]. This compound is stable in alcoholic solutions for more than 6 months, but slowly decomposes in halogenated solvents in daylight. Unlike [{Fe(oepz)}$_2$O], the dimer is very sensitive to inorganic bases. Washing a CH_2Cl_2 solution of [{Fe(oespz)}$_2$O] with 10.0 mol dm^{-3} NaOH led to decomposition of the dimer, whereas treatment with 1.0 mol dm^{-3} NaOH led to a partial conversion of the dimer into the hydroxo derivative, [Fe(oespz)(OH)] (broad ^{1}H NMR signals: a quartet at δ 3.75 assigned to methylene protons, a singlet at δ 1.85 due to the hydroxyl protons and a triplet at δ 1.91 due to the methyl protons). Antiferromagnetic coupling of unpaired electrons through the oxo bridge makes the dimer diamagnetic. Its ^{1}H NMR spectrum shows two partly overlapped double quartets in the range δ 3.95–4.25 assigned, on the basis of the integrated signal, to diastereotopic methylene protons of the ethyl groups, and a triplet at δ 1.91 assigned to the methyl protons.[2b] An intense band at 803.5 cm^{-1} in the IR spectrum, is considered as diagnostic for the asymmetric stretching of the Fe–O–Fe unit.[1] The UV/VIS spectrum of [{Fe(oespz)}$_2$O] shows a not negligible broadening, associated with the π–π interactions within the dimer.[14] We were not able to detect any absorption of the dimer in the NIR region. Treatment of the oxo dimer with aqueous HCl [equation (3)] afforded a dark red crystalline solid formulated and characterized as the [Fe(oespz)Cl] complex.

Crystal structures

The complexes [Mn(oespz)Cl] and [Fe(oespz)Cl] are isostructural. For this reason only the structure of [Mn(oespz)Cl] [Fig. 1(*a*)] will be discussed in detail. The co-ordination geometry around the manganese atom is that of a slightly distorted square pyramid. The displacement of the metal atom out of the planar $(N_p)_4$ (N_p = pyrrolic nitrogen atom) donor set is 0.291(1) Å, ≈0.06 Å longer than in [Mn(tpp)Cl] (tpp = *meso*-5,10,15,20-tetraphenylporphyrinate).[17] The average Mn–N_p distance is

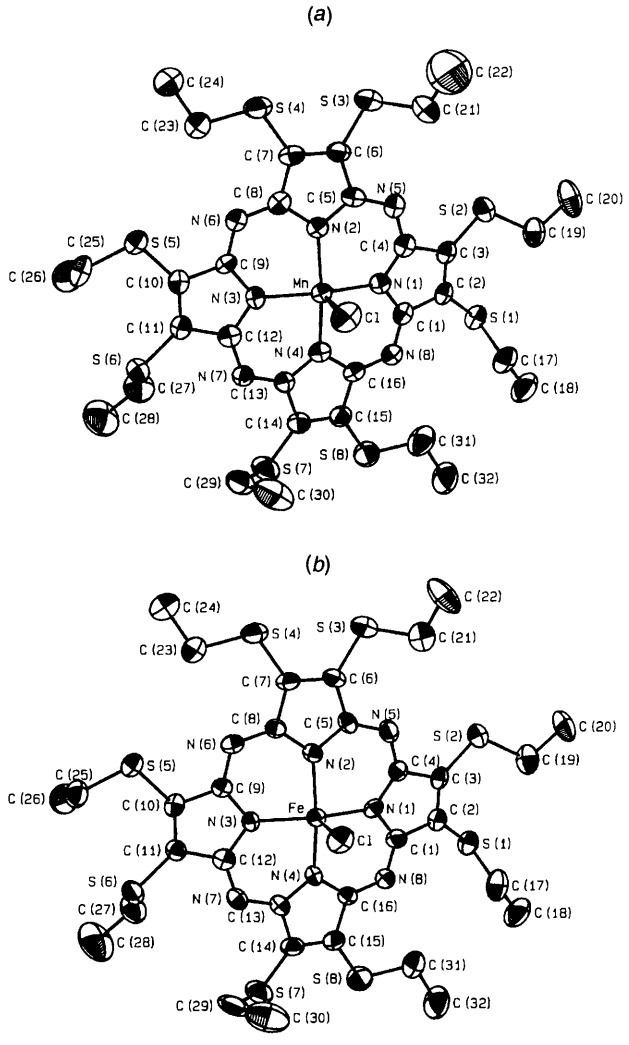

Fig. 1 The ORTEP[16] plots of (*a*) [Mn(oespz)Cl] and (*b*) [Fe(oespz)Cl] with the atom-numbering scheme used; ellipsoids are scaled to enclose 50% of the electron density. Hydrogen atoms are omitted

1.951(6) Å, shorter than that of [Mn(tpp)Cl] (2.02 Å) and of the phthalocyaninato μ-oxo dimer $[Mn_2(pc)_2(py)_2O]$ (py = pyridine) (1.96 Å).[18] The short Mn–N_p distance and the remarkable pyramidalization of the metal-ion geometry are in line with a smaller central hole in the porphyrazines compared to phthalocyanines and porphyrins. The Mn–Cl distance of 2.394 Å is in the range expected for this bond {2.37 and 2.47 Å in [Mn(tpp)Cl] and in [Mn(tpp)Cl(py)]}.[19] The in-plane dimensions of the macrocyclic ring do not differ significantly from the corresponding ones in $[Mg(omspz)(H_2O)]$, nickel and copper *star*-porphyrazines,[2e] [Fe(oepz)Cl] and metallophthalocyanines.[2a] However, as in the peripherally unsubstituted [Fe(oepz)Cl], we note a small but significant contraction of the C_β–C_β bonds with respect to [M(pc)] complexes (average bond length 1.365 *vs.* 1.395 Å).[2a] As for the peripheral ethyl tails, we compute a high thermal parameter for the C(22) atom in the refined structure, probably due to unresolved disorder, a feature already found in the structure of $[Mg(omspz)(H_2O)]$. The crystal packing of [Mn(oespz)Cl] consists of slipped stacks of dimeric units (see Fig. 2). The monomers are slipped within each dimer, in *trans* fashion with respect to the Mn–Cl bond and weakly associated *via* long contacts between Mn and S(1) atom of the adjacent molecule [Mn · · · S(1) 3.231(1) Å] [see Fig. 3(*a*) and (*b*)]. Intradimer interactions at the van der Waals limit also occur between the N(3) and N(4) atoms and the S(1) atom of the adjacent molecule: N(3) · · · S(1) 3.269(7), N(4) · · · S(1) 3.257(8) Å.[21] Owing to the peculiar structure of the

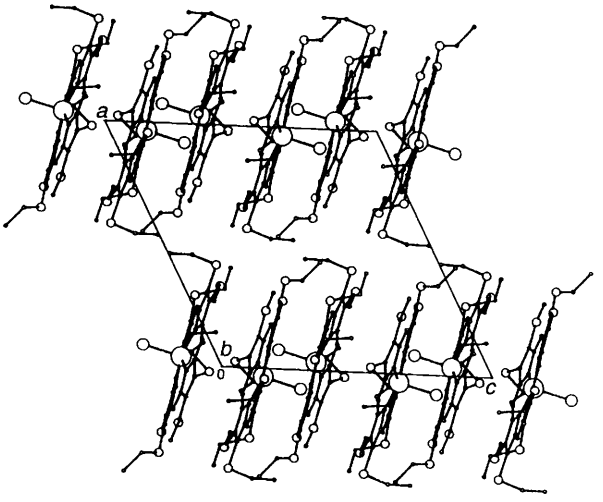

Fig. 2 A PLUTO[20] crystal-packing diagram of [Mn(oespz)Cl]. Hydrogen atoms are omitted for clarity

dimer, the repulsion between the N(3) and N(4) out-of-plane lone pairs and the S(1) lone pair prevents a closer Mn · · · S(1) approach. Along the stack, weak interdimer interactions [3.641(3) Å] arise from S(5) · · · Cl contacts (Cl at $-x, \frac{1}{2}+y, \frac{1}{2}-z$).[21]

Significant out-of-plane molecular distortions induced by the association process can be seen assuming as reference the $(N_p)_4$ planes which are parallel within each dimer and spaced by 3.68(5) Å. With respect to the $(N_p)_4$ plane to which it belongs, the pyrrolic unit involved in the dimerization through the S(1) atom is bent by 7(2)°. The S(1) atom is pushed up, in turn, 0.332(2) Å above the pyrrolic plane and 0.815(2) Å above the $(N_p)_4$ plane. The three remaining pyrrolic units are almost coplanar with the $(N_p)_4$ set and the small displacements of the sulfur atoms from the pyrrolic planes are in line with those found in the structure of $[Mg(omspz)(H_2O)]$. The FAB mass spectral data indicate that the intradimer interactions, though weak, are not negligible. In addition to an isotopic cluster centred at m/z = 847 ($[M - Cl]^+$), there are also peaks of dimeric fragments resulting from the loss of one or two axial chlorine ligands or from their partial demetallation.

As for the [Fe(oespz)Cl] structure [Fig. 1(*b*)] we note that the iron atom is extruded out of the strictly planar $(N_p)_4$ donor set in the direction of the apical chlorine, the distance between the metal atom and the centre of the basal plane being 0.286(1) Å, ≈0.07 Å shorter than that found in [Fe(oepz)Cl]. The average Fe–N_p bond length [1.936(6) Å] is only slightly (≈0.01 Å) longer than in the unsubstituted parent molecule but considerably shorter (0.13 Å) than in [Fe(por)Cl] (por = 3,7,12,17-tetramethyl-8,13-divinylporphyrin-2,18-dipropanoate).[2a] The crystal packing of [Fe(oespz)Cl] consists of stacked dimers where the monomeric units are weakly bound through long contacts between Fe and the S(1) atom of the adjacent molecule [Fe · · · S(1) 3.233(1) Å], and N(3) · · · S(1) 3.255(7), N(4) · · · S(1) 3.247(8) Å. Along the stack weak interdimer interactions [3.637(3) Å] arise from S(5) · · · Cl contacts (Cl at $-x, \frac{1}{2}+y, \frac{1}{2}-z$).[21]

Concerning the peripheral tails, atom C(22) shows disorder. It has been refined in three different positions with fixed occupancy factor of 0.5, 0.25 and 0.25 respectively. As in the case of the manganese complex, the FAB mass spectra of [Fe(oespz)Cl] are indicative of the strength of the intradimer interactions (see Experimental section).

Finally, the structures of [Mn(oespz)Cl] and [Fe(oespz)Cl] show two important features. First, all the intradimer distances lie well above 3.4 Å. As a consequence there is no significant overlap between the π systems of the aromatic rings.[21] Secondly, the dihedral angles relative to the C(ethyl)S$C_\beta C_\beta$ atoms (see

Table 1 Data collection and structure refinement parameters for [Mn(oespz)Cl] and [Fe(oespz)Cl] *

Formula	$C_{32}H_{40}ClMnN_8S_8$	$C_{32}H_{40}ClFeN_8S_8$
M_r	883.63	884.54
a/Å	15.941(2)	15.832(2)
b/Å	18.055(2)	18.039(1)
c/Å	15.797(3)	15.791(2)
β/°	117.71(1)	117.20(1)
U/Å^3	4025.4(8)	4011.0(8)
D_c/g cm^{-3}	1.46	1.46
μ/cm^{-1}	74.3	77.9
$F(000)$	1832	1836
Crystal size/mm	0.19 × 0.12 × 0.16	0.30 × 0.19 × 0.04
2θ Range/°	21.40–25.39	21.61–31.61
h,k,l Ranges	−18 to 17, 0–21, 0–17	−19 to 17, 0–21, 0–18
Unique reflections	6257	7168
Observed reflections [$I > 3\sigma(I)$]	3097	3266
Goodness of fit	3.22	3.25
Maximum Δ/σ	0.12	0.30
Maximum, minimum $\Delta\rho$/e Å^{-3}	0.55, −0.12	0.39, −0.14
R	0.055	0.056
R'	0.059	0.059

* Details in common: monoclinic, space group $P2_1/c$; $Z = 4$; 296 K; 451 parameters; $R = \Sigma(||F_o| - |F_c||)/\Sigma|F_o|$; $R' = [\Sigma w(|F_o| - |F_c|)^2/\Sigma w|F_o|^2]^{\frac{1}{2}}$.

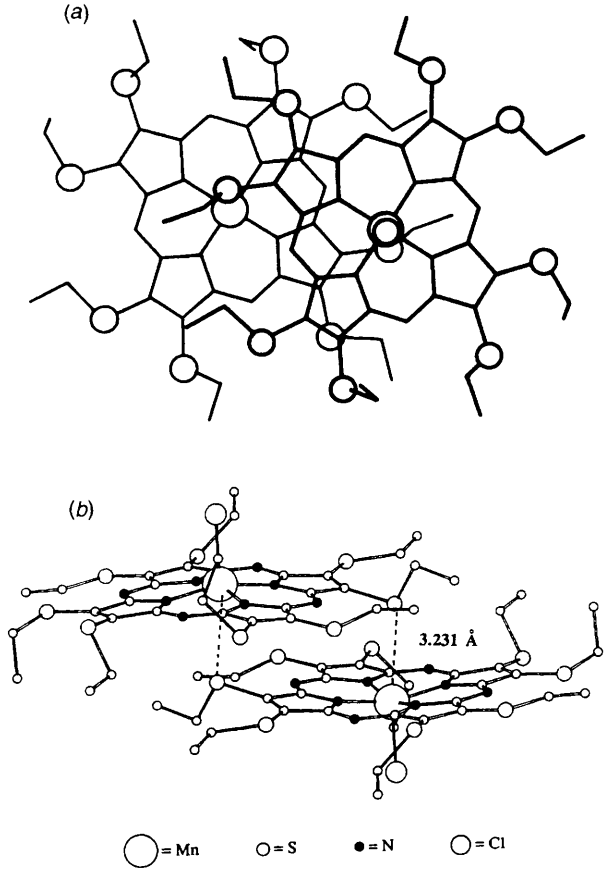

Fig. 3 (*a*) Stick bond model of the [{Mn(oespz)Cl}$_2$] dimer viewed perpendicular to the $(N_p)_4$ mean planes showing the way in which the molecules overlap to give the Mn ··· S(1) interactions. For clarity, only sulfur, manganese and chlorine atoms are drawn as circles. (*b*) A PLUTO edge-on view of [{Mn(oespz)Cl}$_2$] illustrating the slipped-stack arrangement of the monomers and the axial Mn^{III} ··· S(1) contacts. Symmetry operation applied to S(1): $-x, -y, -z$. Hydrogen atoms are omitted for clarity

Tables 2 and 3) span a wide range which implies a possible fluxional behaviour of the peripheral EtS tails.

EPR and magnetic susceptibility data

The nature and the strength of the intradimer interactions account for the solid-state magnetic behaviour of [Mn(oespz)Cl]. The temperature dependence of the magnetic susceptibility measured in the range 2.8–270 K is shown in Fig. 4. At high temperature the value of the effective magnetic moment is 7.0 μ_B as expected for two non-interacting $S = 2$ spins. An $S = 2$ high-spin ground state was also found for [Mn(pc)Cl].[22] The magnetic susceptibility has been computed using the van Vleck equation with the isotropic spin Hamiltonian, $H = JS_1 \cdot S_2$.[23] The experimental data have been fitted using a Simplex minimization routine keeping the electronic Zeeman g factor fixed at 2.00. The computed curve is shown in Fig. 4 as a solid line. The best-fit J value is 1.58(3) cm^{-1} indicating that within each dimer two high-spin manganese(III) ions are weakly antiferromagnetically coupled.

The temperature dependence of the magnetic susceptibility of [Fe(oespz)Cl] measured in the range 2.8–270 K does not show any maximum in the χ *vs.* T curve, indicating that the exchange interactions between the iron centres are smaller than those observed in [Mn(oespz)Cl]. The data have been fitted using a Curie–Weiss equation $\chi = C/(T - \theta)$, the best-fit parameters being $C = 1.62(6)$ cm^3 K mol^{-1} and $\theta = -12.6(8)$ K (-8.76 cm^{-1}). The negative value of θ can be ascribed to either antiferromagnetic interactions between neighbouring spin centres to zero-field splitting effects or to the presence of states having different spin multiplicity populated at the same temperature. In the absence of a maximum we have not tried to fit the data using the model employed for the manganese complex. The measured value of C does not actually correspond to that expected for a iron(III) ion in the high-spin ($S = \frac{5}{2}$, $C = 4.38$ cm^3 K mol^{-1}), low-spin ($S = \frac{1}{2}$, $C = 0.38$ cm^3 K mol^{-1}) or intermediate-spin state ($S = \frac{3}{2}$, $C = 1.9$ cm^3 K mol^{-1}). Also integer spin states originating from a strong exchange interactions between the iron centres are not consistent with the value of C. The above values of C have been computed using the free-electron value, 2.002, for g. In order to obtain more information on the electronic structure of [Fe(oespz)Cl] we have measured the polycrystalline powder EPR spectra. No spectrum was detected at temperatures higher than 20 K. At liquid-helium temperature two sets of intense signals are easily recognized. The first is almost isotropic at $g = 4.3$, the other is rhombic ($S = \frac{1}{2}$) with $g_1 = 2.36$, $g_2 = 2.17$ and $g_3 = 1.96$. A $g = 4.3$ feature is commonly found in many iron(III) spectra and is commonly assigned to species in rhombic environments.[24] Unfortunately, the determination of the absolute intensities of the signals is prevented by their exchange broadening and anisotropy. Nevertheless, the intensity of the $g = 4.3$ signal, although less than that of the other, is not negligible and cannot be ascribed to an impurity. In fact, EPR spectra measured on

Table 2 Selected bond lengths (Å) and angles (°) with estimated standard deviations (e.s.d.s) in parentheses for [Mn(oespz)Cl]. Torsion angles (°) for C(ethylene)$SC_\beta C_\beta$ atoms are also reported

Mn–Cl	2.394(3)	S(7)–C(14)	1.732(7)	N(5)–C(4)	1.330(9)	C(5)–C(6)	1.45(1)
Mn–N(1)	1.947(6)	S(8)–C(15)	1.726(8)	N(5)–C(5)	1.33(1)	C(6)–C(7)	1.38(1)
Mn–N(2)	1.955(5)	N(1)–C(1)	1.370(9)	N(6)–C(8)	1.335(9)	C(7)–C(8)	1.423(9)
Mn–N(3)	1.950(6)	N(1)–C(4)	1.357(8)	N(6)–C(9)	1.314(8)	C(9)–C(10)	1.46(1)
Mn–N(4)	1.955(5)	N(2)–C(5)	1.367(8)	N(7)–C(12)	1.327(9)	C(10)–C(11)	1.367(9)
S(1)–C(2)	1.758(8)	N(2)–C(8)	1.38(1)	N(7)–C(13)	1.31(1)	C(11)–C(12)	1.47(1)
S(2)–C(3)	1.725(7)	N(3)–C(9)	1.367(9)	N(8)–C(1)	1.329(8)	C(13)–C(14)	1.458(9)
S(3)–C(6)	1.739(7)	N(3)–C(12)	1.355(8)	N(8)–C(16)	1.315(9)	C(14)–C(15)	1.36(1)
S(4)–C(7)	1.721(8)	N(4)–C(13)	1.385(9)	C(1)–C(2)	1.46(1)	C(15)–C(16)	1.458(9)
S(5)–C(10)	1.730(8)	N(4)–C(16)	1.39(1)	C(2)–C(3)	1.355(9)	C(17)–C(18)	1.51(1)
S(6)–C(11)	1.740(7)			C(3)–C(4)	1.46(1)		
Cl–Mn–N(1)	100.6(2)	C(1)–N(1)–C(4)	107.2(6)	N(1)–C(1)–C(2)	108.7(5)	S(1)–C(2)–C(3)	129.0(6)
Cl–Mn–N(2)	100.1(2)	C(5)–N(2)–C(8)	106.8(5)	N(2)–C(5)–C(6)	109.5(7)	S(2)–C(3)–C(2)	137.0(6)
Cl–Mn–N(3)	96.6(2)	C(9)–N(3)–C(12)	107.0(6)	N(3)–C(9)–C(10)	109.9(5)	S(3)–C(6)–C(7)	123.8(6)
Cl–Mn–N(4)	96.9(2)	C(13)–N(4)–C(16)	108.2(5)	N(4)–C(13)–C(14)	108.2(6)	S(4)–C(7)–C(6)	122.2(5)
N(1)–Mn–N(2)	88.8(2)	C(4)–N(5)–C(5)	122.1(6)	C(1)–C(2)–C(3)	108.1(6)	S(5)–C(10)–C(11)	137.7(6)
N(1)–Mn–N(4)	88.5(2)	C(8)–N(6)–C(9)	123.2(6)	C(5)–C(6)–C(7)	106.7(6)	S(6)–C(11)–C(10)	130.6(6)
N(2)–Mn–N(3)	88.8(2)	C(12)–N(7)–C(13)	121.5(6)	C(9)–C(10)–C(11)	106.9(6)	S(7)–C(14)–C(15)	126.1(6)
N(3)–Mn–N(4)	88.8(2)	C(1)–N(8)–C(16)	121.7(6)	C(13)–C(14)–C(15)	107.6(6)	S(8)–C(15)–C(14)	122.0(5)
		C(17)–S(1)–C(2)–C(3)	114.3(8)	C(25)–S(5)–C(10)–C(11)	−10.3(1)		
		C(19)–S(2)–C(3)–C(2)	−13.1(1)	C(27)–S(6)–C(11)–C(10)	124.0(8)		
		C(21)–S(3)–C(6)–C(7)	140.9(8)	C(29)–S(7)–C(14)–C(15)	135.8(8)		
		C(23)–S(4)–C(7)–C(6)	180.0(6)	C(31)–S(8)–C(15)–C(14)	−164.2(8)		

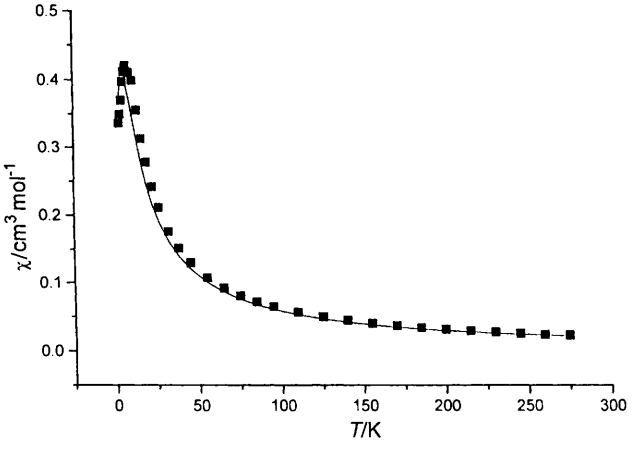

Fig. 4 Temperature dependence of the magnetic susceptibility for [Mn(oespz)Cl]. The solid line is the best fit

different portions of the same sample and on differently prepared samples showed identical features at 4.2 K. Using the EPR results the observed value of the Curie constant, can be rationalized as derived from a mixture of $S = \frac{5}{2}$ and $\frac{1}{2}$ species. Using $g = 2.00$ for the high-spin centre and $g = 2.16$ (average value from the powder spectra) for the low-spin one, a value of $C = 1.62$ cm^3 K mol^{-1} is obtained for a mixture formed by 70% of the low-spin and 30% of the high-spin species.

In order to see whether the solid-state structure can influence the spin state of [Fe(oespz)Cl] we have measured its frozen-solution EPR spectra. The toluene solution frozen-glass EPR spectrum at 77 K exhibits a sharp signal attributable to an effective axially symmetric $S = \frac{1}{2}$ species.[2a] The $g_\perp$ and $g_\parallel$ values are respectively 3.92 and 1.96, very similar to those measured for the unsubstituted complex [Fe(oepz)Cl] ($g_\perp$ = 3.96 and $g_\parallel$ = 1.92). The experimental g values for the latter were rationalized in terms of a pure $S = \frac{3}{2}$ ground state.[2a] The substantial agreement of the EPR spectrum of [Fe(oespz)Cl] with that of its unsubstituted parent seems to point to an $S = \frac{3}{2}$ ground state also for [Fe(oespz)Cl] in solution.

The EPR results seem to indicate that the spin state of the Fe^{III} in [Fe(oespz)Cl] is rather sensitive to the actual environment of the complex. The frozen-solution spectra show that, in the absence of interactions, Fe^{III} possesses a $S = \frac{3}{2}$ ground state. In the solid state the axial interactions and the distortions of the metal co-ordination sphere [Cl–Fe–S(1) 165° at room temperature] probably lead to an electronic structure in which the high- and low-spin electronic states are similar in energy. Based on the substantial constancy of the unit-cell parameters measured for several crystals also from different sample batches, we can exclude, a polymorphic behaviour for [Fe(oespz)Cl]. Nevertheless, at low temperature, changes in the intermolecular arrangement may still occur, although this does not show up in the shape of the magnetic susceptibility curve. Low-temperature reinforcement of Fe–S axial interaction has been measured in iron(III) porphyrin complexes with axial thioether ligation.[25] Similarly, both high- and low-spin EPR signals and a temperature-dependent ground spin state are observed for those complexes.

UV/VIS/NIR spectroscopy

The UV/VIS spectrum of [Mn(oespz)Cl] is compared in Fig. 5(*a*) with that of [Mn(pc)Cl]. The spectrum of [Mn(oespz)Cl] features two intense absorptions, at 350 and at 720 nm, ascribed to the Soret and Q bands. The Q band is nearly coincident with that of [Mn(pc)Cl], whereas the Soret band is blue-shifted. The region ranging from 450 to 600 nm in the [Mn(oespz)Cl] spectrum is rather crowded as a result of a number of transitions comprising the higher-energy components of the Q band, the charge-transfer absorptions involving the sulfur lone pairs and absorption splittings due to association phenomena. Both the position and intensity of the bands spanning this range show a dependence on the solvent and concentration (the Lambert–Beer law is not followed when $c \geqslant 5 \times 10^{-5}$ mol dm^{-3}). Three absorptions are found in the NIR region, at ≈890, 1120 and 1350 nm, in chloroform. These are less intense than those of [Mn(por)Cl] and [Mn(pc)Cl] in the same region.[26] Their apparent solvatochromism [see Fig. 5(*b*)] seems, furthermore, to point to a ligand-to-metal charge-transfer (l.m.c.t.) nature.

The UV/VIS spectrum of [Fe(oespz)Cl], shown in Fig. 6(*a*), exhibits a moderately intense absorbance at the visible–NIR border (700–870 nm) which is accompanied by a higher-energy (≈600 nm) intense band (Q band). In the 400–550 nm region two not well resolved and intense peaks are found, while at 320

Table 3 Selected bond lengths (Å) and angles (°) with e.s.d.s in parentheses for [Fe(oespz)Cl]. Torsion angles (°) for C(ethylene)$SC_{\beta}C_{\beta}$ atoms are also reported

Fe–Cl	2.308(3)	S(7)–C(14)	1.735(7)	N(5)–C(4)	1.312(9)	C(5)–C(6)	1.43(1)
Fe–N(1)	1.934(6)	S(8)–C(15)	1.722(8)	N(5)–C(5)	1.35(1)	C(6)–C(7)	1.37(1)
Fe–N(2)	1.939(5)	N(1)–C(1)	1.365(9)	N(6)–C(8)	1.331(9)	C(7)–C(8)	1.425(9)
Fe–N(3)	1.941(6)	N(1)–C(4)	1.365(8)	N(6)–C(9)	1.311(8)	C(9)–C(10)	1.47(1)
Fe–N(4)	1.932(5)	N(2)–C(5)	1.357(8)	N(7)–C(12)	1.318(9)	C(10)–C(11)	1.364(9)
S(1)–C(2)	1.741(8)	N(2)–C(8)	1.357(9)	N(7)–C(13)	1.35(1)	C(11)–C(12)	1.47(1)
S(2)–C(3)	1.720(7)	N(3)–C(9)	1.364(9)	N(8)–C(1)	1.324(8)	C(13)–C(14)	1.439(9)
S(3)–C(6)	1.739(7)	N(3)–C(12)	1.371(8)	N(8)–C(16)	1.320(9)	C(14)–C(15)	1.36(1)
S(4)–C(7)	1.743(8)	N(4)–C(13)	1.354(8)	C(1)–C(2)	1.46(1)	C(15)–C(16)	1.469(9)
S(5)–C(10)	1.737(7)	N(4)–C(16)	1.389(9)	C(2)–C(3)	1.378(9)	C(17)–C(18)	1.51(1)
S(6)–C(11)	1.736(7)			C(3)–C(4)	1.48(1)		
Cl–Fe–N(1)	100.2(2)	C(1)–N(1)–C(4)	107.6(6)	N(1)–C(1)–C(2)	110.0(5)	S(1)–C(2)–C(3)	128.6(6)
Cl–Fe–N(2)	99.3(2)	C(5)–N(2)–C(8)	105.9(5)	N(2)–C(5)–C(6)	111.5(6)	S(2)–C(3)–C(2)	136.6(6)
Cl–Fe–N(3)	97.1(2)	C(9)–N(3)–C(12)	106.8(6)	N(3)–C(9)–C(10)	109.8(5)	S(3)–C(6)–C(7)	123.9(6)
Cl–Fe–N(4)	97.3(2)	C(13)–N(4)–C(16)	106.4(5)	N(4)–C(13)–C(14)	111.5(7)	S(4)–C(7)–C(6)	121.6(5)
N(1)–Fe–N(2)	88.7(2)	C(4)–N(5)–C(5)	120.8(6)	C(1)–C(2)–C(3)	106.6(6)	S(5)–C(10)–C(11)	137.5(6)
N(1)–Fe–N(4)	88.9(2)	C(8)–N(6)–C(9)	121.6(6)	C(5)–C(6)–C(7)	105.2(6)	S(6)–C(11)–C(10)	131.2(6)
N(2)–Fe–N(3)	88.5(2)	C(12)–N(7)–C(13)	121.2(6)	C(9)–C(10)–C(11)	107.2(6)	S(7)–C(14)–C(15)	125.8(6)
N(3)–Fe–N(4)	88.9(2)	C(1)–N(8)–C(16)	121.0(6)	C(13)–C(14)–C(15)	106.3(6)	S(8)–C(15)–C(14)	122.9(5)
		C(17)–S(1)–C(2)–C(3)	116.5(8)	C(25)–S(5)–C(10)–C(11)	−10.6(1)		
		C(19)–S(2)–C(3)–C(2)	−11.1(1)	C(27)–S(6)–C(11)–C(10)	122.7(8)		
		C(21)–S(3)–C(6)–C(7)	145.4(9)	C(29)–S(7)–C(14)–C(15)	−135.53(8)		
		C(23)–S(4)–C(7)–C(6)	177.5(8)	C(31)–S(8)–C(15)–C(14)	−167.1(8)		

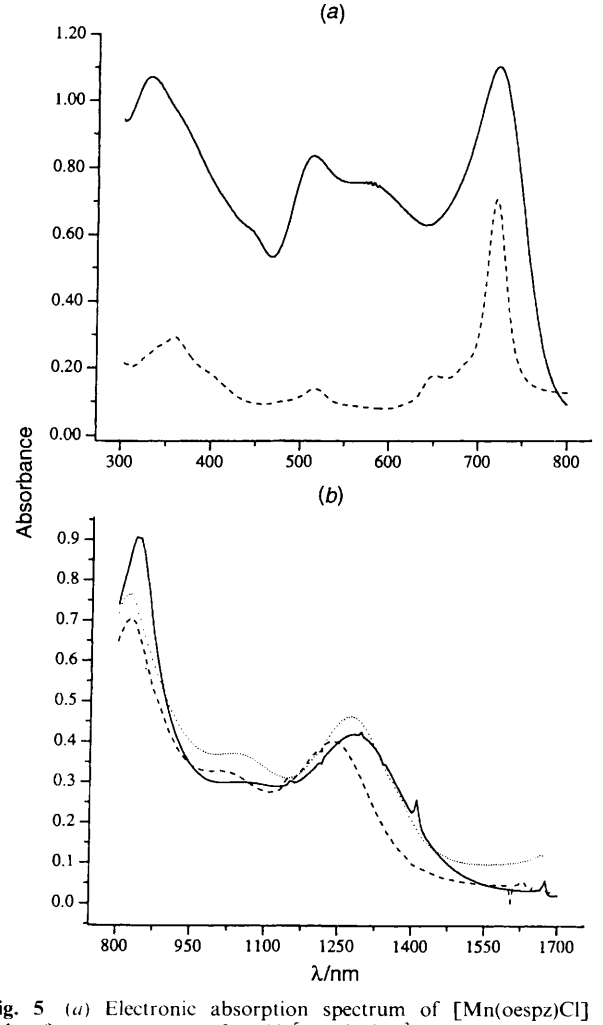

Fig. 5 (*a*) Electronic absorption spectrum of [Mn(oespz)Cl] in chloroform (——), $c = 3 \times 10^{-5}$ mol dm^{-3}, and [Mn(pc)Cl] in chlorobenzene (– – –) in the region 300–800 nm, $c = 4.7 \times 10^{-6}$ mol dm^{-3}. (*b*) The NIR absorption spectrum of [Mn(oespz)Cl] in chloroform (——), dmf (· · ·) and toluene (– – –), $c = 10^{-4}$ mol dm^{-3}. Cell path length = 10 cm

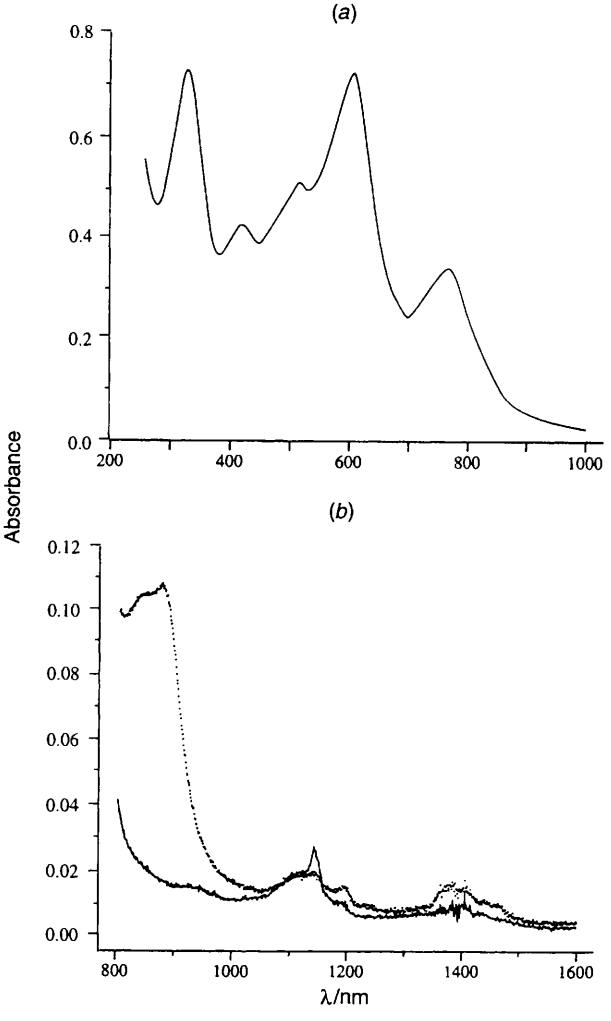

Fig. 6 (*a*) Electronic absorption spectrum of [Fe(oespz)Cl] in the region 250–1000 nm, $c = 2 \times 10^{-5}$ mol dm^{-3}. (*b*) The NIR absorption spectrum of [Fe(oespz)Cl] in chloroform (——) and in dmf (· · ·), $c = 10^{-4}$ mol dm^{-3}, cell path length = 10 cm

nm the almost symmetric shape of the intense Soret (B) band is clearly discernible. A red shift ($\approx$100 nm) of the Q band and a considerable crowding of the region between the Q and the B band are noted when comparing the spectrum of [Fe(oespz)Cl] with that of the unsubstituted parent, [Fe(oepz)Cl]. Unlike mononuclear iron(III) phthalocyanines, [Fe(oespz)Cl] exhibits NIR absorptions [see Fig. 6(*b*)]. Two relatively weak absorptions are noted at 950 ($\varepsilon \approx 250$) and 1130 nm ($\varepsilon \approx 300$ $dm^3\ mol^{-1}\ cm^{-1}$) in non-co-ordinating solvents, and a weak band at $\approx$1400 nm ascribed to combination and overtone C–H bending.[2h] Noteworthily, in dmf there is a twin absorption with maxima at 880 and 920 nm having increased intensity (ε = 1250 $dm^3\ mol^{-1}\ cm^{-1}$) compared to the other two bands centred at 1130 and 1400 nm. This behaviour seems reminiscent of that of iron(III) phthalocyanine.[27]

Electrochemistry

The electrochemical behaviour of [Mn(oespz)Cl] and [Fe(oespz)Cl] has been studied by cyclic voltammetry. The former exhibits a reversible wave with $E_{\frac{1}{2}} = 0.055$ V [see Fig. 7(*a*)]. The wave has to be ascribed to the Mn^{III}–Mn^{II} couple, as it lies midway between that of the first oxidation ($E_{pa} = 0.850$ V) and that of the first reduction ($E_{\frac{1}{2}} = -0.450$ V *vs.* Ag–AgCl) of H_2oespz. The half-wave potential of the couple is at least 50 and 400 mV more anodic than those of manganese phthalocyanines and [Mn(tpp)Cl],[28] indicating that the octa(alkylsulfanyl)porphyrazines strongly stabilize the lower oxidation state of the co-ordinated manganese atom relative to phthalocyanines and porphyrins. Further stabilization of the manganese(II) state is induced by the interaction with a sixth donor ligand as indicated by the anodic shift of the potential of the Mn^{III}–Mn^{II} couple to 0.075 and 0.100 V in the presence of pyridine and 1-methylimidazole respectively.[29] A similar effect is noted when the Cl^- counter ion is replaced by ClO_4^- ($E_{\frac{1}{2}} = 0.125$ V) or BF_4^- ($E_{\frac{1}{2}} = 0.115$ V).[27,30,31] The first reduction wave, which is also fully reversible, lies at -0.470 V and is independent of solvent or counter ion. Taken together with the Nernstian character of the wave, this might be indicative of a redox process leading to the $[Mn^{II}\{oespz(3-)\}]^-$ radical anion. Spectroelectrochemical studies on the first reduction wave of [Mn(pc)] show that the formation of a radical anion is a real process.[27,30,31] The cathodic part of the voltammogram of [Mn(oespz)Cl] ranging from -0.7 to -1.9 V (not shown) exhibits, in CH_2Cl_2, three further waves, the nature and positions of which depend on the solvent and counter ion. In the absence of spectroscopic and/or magnetic confirmatory data we did not attempt to assign them. The complex [Mn(oespz)Cl] in dichloromethane does not exhibit any redox process in the region 0.2–1.3 V.

The voltammogram of [Fe(oespz)Cl] in CH_2Cl_2 is featureless. Addition of 1 or 2 equivalents of pyridine to the solution affords five redox processes [Fig. 7(*b*)] in the range 1.4 to -1.7 V. The complex undergoes a fully reversible process to be ascribed to the Fe^{III}–Fe^{II} couple at $E_{\frac{1}{2}} = +0.170$ V. This value is very close to that obtained, under similar conditions, for the same couple, for [Fe(oepz)].[2a] In the region 0 to -1.7 V the voltammogram shows an irreversible reduction wave with $E_{c1} = -0.95$ V, $\Delta(E_{c1} - E_{a1}) = 150$ mV and a quasi-reversible one with $E_{c2} = -1.40$ V, $\Delta(E_{c2} - E_{a2}) = 90$ mV. These values are cathodic of those exhibited by free base and (methylsulfanyl)porphyrazine derivatives of Cu, Co, Ni and Zn.[3] The first and second reduction waves are separated by 0.39 V, a value comparable with that reported for the free base (0.33 V), metallo(alkylsulfanyl)porphyrazines ($\approx$0.36 V) and metallophthalocyanines (0.4 V).[3] This seems to be consistent with sequential reduction of the oespz ring. Interestingly, the first reduction becomes chemically and electrically reversible when the potential scan is reversed at -1.2 V. The molecule undergoes two oxidations at $E_{a1} = 0.79$ and $E_{a2} = -0.95$ V

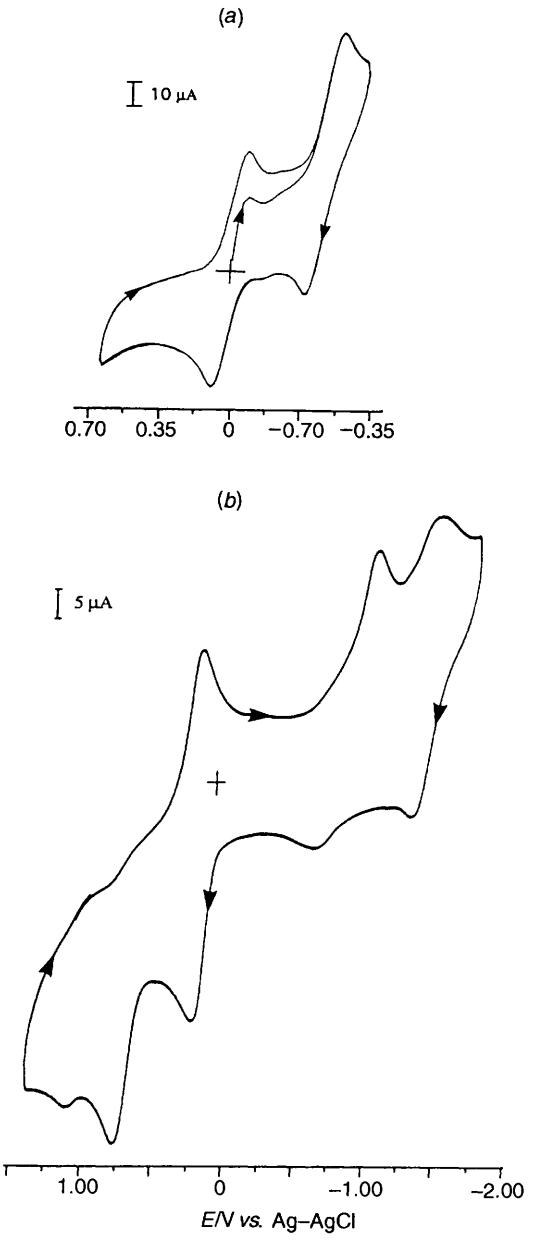

Fig. 7 Cyclic voltammograms of (*a*) [Mn(oespz)Cl] in the range 0.7 to -0.7 V in CH_2Cl_2–0.1 mol dm^{-3} $[NBu^n_4]Cl$, $c = 5 \times 10^{-5}$ mol dm^{-3}, scan rate = 100 mV s^{-1} and (*b*) [Fe(oespz)Cl] in CH_2Cl_2–0.1 mol dm^{-3} $[NBu^n_4][BF_4]$, $c = 10^{-4}$ mol dm^{-3}, scan rate = 100 mV s^{-1}, [pyridine] = 2×10^{-4} mol dm^{-3}, from 0.3 to -1.7 to 1.4 to 0.3 V

which have only a weak cathodic counterpart indicating that the oxidized products, as occurs with metallophthalocyanines, are highly reactive species.[27]

Conclusion

We have reported the synthesis, structure and a physicochemical characterization of octa(ethylsulfanyl)porphyrazines of Mn^{III} and Fe^{III}. The structure of both complexes is peculiar in that it exhibits the longest $M^{III}\cdots S$ axial interaction observed in a porphyrin-like complex.

Additional intermolecular $M\cdots S$ contacts very similar ($\geqslant$3.38 Å) to those described in this paper were found to occur in the mesogenic complexes of Ni^{II}, Pd^{II} and Hg^{II} with 4-alkoxydithiobenzoates.[32] Concerning manganese(III) porphyrin-like complexes, $[MnL(MeOH)]BPh_4$ [H_2L = 4-benzylsulfanyl-2-methyl-*N*,*N*′-bis(salicylidene)butane-1,2-diamine] is the only one showing an Mn^{III} weakly bound to a thioether group [$Mn\cdots S$ 2.798(1) Å] in a pseudo-octahedral

environment.[29] In turn, the Fe···S distance within the [{Fe(oespz)Cl}$_2$] dimer is considerably longer than that in iron(III) porphyrins with axial thioether ligation, such as [Fe(tpp)(tht)$_2$][ClO$_4$] (tht = tetrahydrothiophene), where Fe–S$_{ax}$ is 2.357(27) Å.[25a,c] As inferred from FAB mass spectral data, the Mn···S and Fe···S interactions, though weak, are not negligible. For this reason they might be responsible for the solid-state magnetic behaviour of [Mn(oespz)Cl] and [Fe(oespz)Cl].

Notably the observed stacking pattern of the monomeric units in the dimer prevents any direct contact between the porphyrazinato cores, the only ligand–ligand intradimer interactions being restricted to the S(1) and N(3) and N(4) atoms of the adjacent molecule. The Mn···S and Fe···S axial interactions are of bioinorganic interest, since they mimic the approach of methionine to cytochrome c.[25a-c]

Besides their ability to enable axial metal–ligand interactions, the peripheral thioether groups have electronic structure effects which are specially evident in the electronic absorption spectra of [Mn(oespz)Cl] and [Fe(oespz)Cl]. The electrochemical properties, on the contrary, are only slightly influenced by the presence of the thioether groups at the periphery of the porphyrazinato ring, as shown by the apparent closeness of the redox potential of the Fe^{III}–Fe^{II} couple in [Fe(oespz)Cl] and in its unsubstituted parent. In the case of [Mn(oespz)Cl] the redox potential of the Mn^{III}–Mn^{II} couple may be compared only to that measured for manganese phthalocyanines and porphyrins. The notable anodic shift of the potential is clearly in line with the general tendency of porphyrazines to stabilize the Mn^{II} *vs.* Mn^{III} oxidation state through a more effective metal to ligand π-back donation.[2a]

Acknowledgements

Thanks are expressed to Dr. A. Caneschi, University of Firenze, for performing magnetic measurements, to the Servizio di Spettrometria di Massa, University of Napoli, for FAB mass spectra and to Professor P. Pucci for helping in their interpretation, to Mr. S. Laurita for collecting X-ray data and to Mr. C. Barlabà for technical support. Financial support from Ministero della Università e della Ricerca Scientifica e Tecnologica (MURST) and from Consiglio Nazionale delle Ricerche (CNR) is also gratefully acknowledged.

References

1 N. Kobayashi, in *Phthalocyanines, Properties and Applications*, eds. C. C. Leznoff and A. B. P. Lever, VCH, New York, 1993, vol. 2, p. 97.
2 (*a*) J. Fitzgerald, B. S. Haggerty, A. N. Rheingold and L. May, *Inorg. Chem.*, 1992, **31**, 2006; (*b*) N. Yaping, J. Fitzgerald, P. Carroll and B. B. Wayland, *Inorg. Chem.*, 1994, **33**, 2029; (*c*) A. Ghosh, J. Fitzgerald, P. G. Gassman and J. Almlof, *Inorg. Chem.*, 1994, **33**, 6057; (*d*) C. J. Schramm and B. M. Hoffman, *Inorg. Chem.*, 1980, **19**, 383; (*e*) C. S. Velázquez, G. A. Fox, W. E. Broderick, K. A. Andersen, O. P. Anderson, A. G. M. Barrett and B. M. Hoffman, *J. Am. Chem. Soc.*, 1992, **114**, 7416; (*f*) F. Bonosi, G. Ricciardi, F. Lelj and G. Martini, *J. Phys. Chem.*, 1993, **97**, 9181; (*g*) F. Bonosi, G. Ricciardi, F. Lelj and G. Martini, *J. Phys. Chem.*, 1994, **98**, 10 613; (*h*) G. Ricciardi, F. Lelj and F. Bonosi, *Chem. Phys. Lett.*, 1993, **215**, 541; (*i*) F. Bonosi, F. Lelj, G. Ricciardi and G. Martini, *Thin Solid Films*, 1994, **243**, 335; (*j*) F. Bonosi, G. Ricciardi and F. Lelj, *Thin Solid Films*, 1994, **243**, 310; (*k*) F. Lelj, G. Morelli, G. Ricciardi, A. Roviello and A. Sirigu, *Liq. Cryst.*, 1992, **12**, 6, 941.
3 N. Kobayashi, S. Nakajima and T. Osa, *Chem. Lett.*, 1992, **12**, 241S-18 and refs. therein; G. Ricciardi and F. Lelj, unpublished work.
4 S. H. Strauss, *Chemtracts-Inorg. Chem.*, 1994, **6**, 1.
5 S. A. Hudson and P. M. Maitlis, *Chem. Rev.*, 1993, **93**, 861; N. Kobayashi, in *Phthalocyanines, Properties and Applications*, eds. C. C. Leznoff and A. B. P. Lever, VCH, New York, 1993, vol. 2, p. 253 and refs. therein.
6 D. D. Perrin and W. L. F. Armarego, *Purification of Laboratory Chemicals*, 3rd edn., Pergamon, Oxford, 1988.
7 N. Walker and D. Stuart, *Acta Crystallogr., Sect. A*, 1983, **39**, 159.
8 P. Main, S. J. Fiske, S. E. Hull, L. Lessinger, G. Germain, J.-P. Declercq and M. M. Wolfson, MULTAN 80, Universities of York and Louvain, 1980.
9 *International Tables for X-Ray Crystallography*, Kynoch Press, Birmingham, 1974, vol. 4, p. 99.
10 C. K. Fair, MOLEN, Structure Determination System, Delft, 1990.
11 M. J. Camenzind and C. L. Hill, *Inorg. Chim. Acta*, 1985, **99**, 63.
12 H. U. Blaser and J. Halpern, *J. Am. Chem. Soc.*, 1980, **102**, 1684.
13 D. Lexa, J. Mispelter and J.-M. Saveant, *J. Am. Chem. Soc.*, 1981, **103**, 6806.
14 K. Kim, W. S. Lee, H.-J. Kim, S.-H. Cho, G. S. Girolami, P. A. Gorlin and K. S. Suslick, *Inorg. Chem.*, 1991, **30**, 2652 and refs. therein.
15 D. Astruc, in *Electron Transfer and Radical Processes in Transition-metal Chemistry*, VCH, New York, 1995, p. 325 and refs. therein.
16 C. K. Johnson, ORTEP, Report ORNL-5138, Oak Ridge National Laboratory, Oak Ridge, TN, 1976.
17 L. J. Boucher, in *Coordination Chemistry of Macrocyclic Compounds*, ed. G. A. Melson, Plenum, New York, 1979, p. 527 and refs. therein.
18 L. H. Vogt, A. Zalkin and D. H. Templeton, *Inorg. Chem.*, 1967, **6**, 1725.
19 D. Koenig, *Acta Crystallogr.*, 1965, **18**, 663.
20 W. O. S. Motherwell and W. Clegg, PLUTO 78, Program for plotting molecular and crystal structures, University of Cambridge, 1978.
21 L. Pauling, in *The Nature of the Chemical Bond*, 3rd edn., Cornell University Press, Ithaca, NY, 1960.
22 J. F. Meyers, G. W. Rayner-Canham and A. B. P. Lever, *Inorg. Chem.*, 1981, **14**, 461.
23 O. Khan, *Molecular Magnetism*, VCH, New York, 1993.
24 J. R. Pilbrow, in *Transition Ion Electron Paramagnetic Resonance*, Clarendon Press, Oxford, 1990.
25 (*a*) T. Mashiko, C. A. Reed, K. J. Haller, M. E. Kastner and W. R. Scheidt, *J. Am. Chem. Soc.*, 1981, **103**, 5758; (*b*) J. McKnight, M. R. Cheesman, C. A. Reed, R. D. Orosz and A. J. Thomson, *J. Chem. Soc., Dalton Trans.*, 1991, 1887; (*c*) S. Karmakar, S. B. Choudhury and A. Chakravorty, *Inorg. Chem.*, 1994, **33**, 6148; (*d*) P. H. Rieger, *Coord. Chem. Rev.*, 1994, **135**, 203.
26 L. Boucher, *Coord. Chem. Rev.*, 1972, **7**, 289.
27 A. B. P. Lever, S. R. Pickens, P. C. Minor, S. Licoccia, B. S. Ramaswamy and K. Magnell, *J. Am. Chem. Soc.*, 1981, **103**, 6800.
28 F. A. Schultz, in *Molecular Electrochemistry of Inorganic, Bioinorganic and Organometallic Compounds*, NATO ASI C385, eds. A. J. L. Pombeiro and J. A. McCleverty, Kluwer, Dordrecht, 1993, p. 179 and refs. therein.
29 M. Tomita, N. Matsumoto, H. Akagi, H. Okawa and S. Kida, *J. Chem. Soc., Dalton Trans.*, 1989, 179.
30 A. B. P. Lever, P. C. Minor and J. P. Wilshire, *Inorg. Chem.*, 1981, **20**, 2550.
31 A. B. P. Lever and P. C. Minor, *Adv. Mol. Relaxation Processes*, 1980, **18**, 115.
32 A.-M. Giroud-Godquin and P. M. Maitlis, *Angew. Chem., Int. Ed. Engl.*, 1991, **30**, 375.

Received 22nd *February* 1996; *Paper* 6/01288D